Channel Formation in Gels

N. G. Cogan*

James P. Keener†

*Department of Mathematics, Tulane University, New Orleans, La. E-mail: cogan@math.tulane.edu FAX:504 865 5063

†Department of Mathematics, University of Utah, Salt Lake City, Ut. E-mail: keener@math.utah.edu FAX:801 581 4148

Abstract

We derive a model of gel dynamics based on a two-phase description of the gel where one phase consists of networked polymer and the second phase is the fluid solvent. We describe the treatment of the chemical structure of polymer network and the non-Newtonian stress on the network. The model is used to analyse the dynamics of a gel forced to move between two flat plates by a pressure gradient. The distribution of the network phase is shown to be nonuniform and dependent on the pressure drop. There is a range of pressure gradients for which the network has regions of high and low volume fraction separated by a sharp boundary.

Keywords: gel, model, viscoelasticity, osmotic pressure, biofilm

AMS Subject Classifications: 74D99, 74G10, 76T99

1 Introduction

There are numerous biological and biotechnological examples where the structure and dynamics of polymer gels regulates the local environment. Biological examples include maintenance of structural integrity in biofilms [7], cellular cytoplasm [3], force generators in Myxobacteria [13], chemical diffusion and adsorption mediation in biofilm clusters [11]. Gel patches and ingestible pills used to regulate the diffusion and adsorption of drugs are examples of bioengineered gels. Quantifying the role of the polymer gel in such diverse systems requires understanding the effect of the physical and chemical structure of the polymers on the material properties of the system.

Gels are composed of a polymer network and a fluid solvent. This composition endows gels with properties different than those of viscous materials for two primary reasons. First, the polymeric structure induces viscoelastic behavior such as creep, relaxation and shear thinning. Second, the chemical structure of the polymer induces force causing gel swelling and de-swelling. In this paper we first introduce a two-phase description of gel dynamics that emphasizes these two important differences between gels and Newtonian fluids. The behavior of a pressure driven gel between two flat plates is analyzed in a manner similar to

the standard Poiseulle flow problem. Results from this analysis indicate that the steady-state network profile depends on the pressure gradient in a relatively complicated manner. There is an intermediate range of pressure gradients for which the majority of the network compressed and is located near the plates creating a channeled region which is relatively free of polymer. This channeled solution bifurcates from a nearly uniform network distribution by forming a deep, narrow channel.

2 A Model of Gel Dynamics

Gels consist of two materials, networked polymer and fluid solvent, where the network encapsulates the solvent. The polymer network can be formed by several different interactions between the polymers themselves including covalent bonding, coulombic bonding, hydrogen bonding and physical entanglement.

In response to external conditions gel networks absorb or expel solvent causing swelling or contraction respectively. Thus the structure of the gel depends on the temperature, solvent composition, pH, hydrostatic pressure and ionic concentrations. The potential which is responsible for the swelling properties of the gel is referred to as osmotic or swelling pressure.

Forces due to osmotic pressure are not the only forces acting on the polymer network. Deformation of the gel induces forces due to the elastic nature of the polymer network. The elasticity is caused by both the elasticity of the polymers themselves and polymer interactions. That is, a single polymer acts as a spring for small deformations while entanglement and cross-linking causes the network to resist deformations. The behavior is in general not well described by a simple linear relationship between displacement (strain) and stress primarily because the deformations are typically large.

Because the cross-links may be broken, a strain imposed on the gel and held induces a stress which dissipates, a process referred to as relaxation. Further, if a fixed stress is imposed on the gel, the gel will continue to displace, which is referred to as creep. The two behaviors of creep and relaxation indicate that gels are viscoelastic materials, therefore the constitutive relationship between stress and strain is more complicated than for viscous

materials.

Here we assume that a gel is composed of two immiscible materials, polymer network and fluid solvent. The resulting model is similar to other models [3, 5, 8, 10, 12] that describe the gel as a two-phase material. The primary variation among models in the literature results from the treatment of the viscoelastic stress and the swelling pressure.

In the following sections we describe a general model of gel dynamics and specify the forms of the viscoelastic stress and osmotic pressure used in this investigation. The resulting model is then used to study the distribution of the polymer network when the gel is forced to move between two flat plates by a pressure gradient.

2.1 Model Derivation

We consider a region of space that contains networked polymer and solvent, where the volume fraction of network, θ_n, and the volume fraction of solvent, θ_s, sum to one. The network is assumed to act as a constant density, viscoelastic material while the solvent acts as a Newtonian fluid of much less viscosity than the networked material. The velocities of network and solvent are denoted $\vec{U}_n$ and $\vec{U}_s$ respectively.

The equation describing the momentum of the polymer network is given by the balance of four forces that act on the network. Surface forces are given by $\nabla \cdot (\theta_n \sigma_n)$, where σ_n is the network stress tensor. We assume that $\sigma_n = \sigma_v + \sigma_e$ where the viscous and viscoelastic stresses are denoted σ_v and σ_e respectively. The viscous stress tensor is proportional to the velocity gradient, $\sigma_v = \eta(\nabla \vec{U}_n + \nabla \vec{U}_n^{\,T})$. The non-Newtonian stress tensor is given by constitutive relations which depend on the material and flow regimes [1]. Here we take the elastic stress to be proportional to the elastic strain which is determined by the displacement gradient. We do not allow for creep or relaxation of stress. Since the displacements are not small, we use a finite strain tensor. The displacement of a fluid particle relative to fixed Eulerian coordinates is determined by

$$\vec{x}' = \vec{x} + \vec{D}(\vec{x}, t),$$

where $\vec{x}'$ denotes the past position of the fluid particle and the components of the vector $\vec{D}$

are the displacements.

Following the development given in [1], we relate the stress to the relative Cauchy strain tensor

$$\mathbf{C}(\vec{x},t)_{i,j} = \frac{\partial x'_j}{\partial x_i}\frac{\partial x'_i}{\partial x_j} - \delta_{ij},$$

where $\mathbf{F}_{ij} = \frac{\partial x'_i}{\partial x_j}$ is the deformation gradient tensor and $\delta_{ij} = 0$ if $i \neq j$.

We must also specify equations describing the change in displacements due to advection. The time derivative is measured in convected coordinates (i.e., relative to a fixed coordinate system). We assume that the gel is an elastic solid with rest position at which there is no network strain while displacements from rest induce a strain on the network. Relaxation of the network has been ignored since we are primarily interested in coupling between elastic stress and network motion. Thus

$$\frac{\partial}{\partial t}\vec{D} + \nabla\cdot(\vec{D}\vec{U_n}) = \vec{U_n}. \tag{1}$$

The motion of the solvent influences the network through frictional drag which we model by $h_f\theta_n\theta_s(\vec{U_n} - \vec{U_s})$, where $\vec{U_n}$ and $\vec{U_n}$ are the network and solvent velocities and h_f is the constant coefficient of friction.

The third force is induced by the chemically active nature of the polymers within the gel. To model this force, we assume that there exists an osmotic pressure, $\Psi(\theta)$, gradients of which introduce force on the polymers. Additional description of this term is provided below.

The final force that is included is due to hydrostatic pressure, P. Balancing these forces yields

$$\begin{aligned} \nabla\cdot(\theta_n\sigma_n) - h_f\theta_n\theta_s(\vec{U_n} - \vec{U_s}) & \\ -\nabla\Psi(\theta_n) - \theta_n\nabla P &= 0. \end{aligned} \tag{2}$$

The equation governing the solvent momentum is derived in a similar manner. However, the fluid is chemically passive so there is no osmotic force on the solvent and the stress is

Newtonian. Also, because the viscosity of the fluid is assumed to be much less than that of the network, we neglect the viscous stress. Force balance yields

$$h_f \theta_n \theta_s (\vec{U}_n - \vec{U}_s) - \theta_s \nabla P = 0. \tag{3}$$

The redistribution of polymer network is governed by the conservation equation

$$\frac{\partial}{\partial t}\theta_n + \nabla \cdot (\theta_n \vec{U}_n) = 0, \tag{4}$$

and a similar equation governs the conservation of solvent, namely

$$\frac{\partial}{\partial t}\theta_s + \nabla \cdot (\theta_s \vec{U}_s) = 0. \tag{5}$$

Assuming that $\theta_n + \theta_s = 1$, we combine (4) and (5) to conclude that the divergence of the average flow, $\theta_n \vec{U}_n + \theta_s \vec{U}_s$, is zero, i.e. ,

$$\nabla \cdot (\theta_n \vec{U}_n + \theta_s \vec{U}_s) = 0. \tag{6}$$

The equations 1, 2, 3, 4 and 6 define the equations which govern the gel dynamics, subject to boundary conditions which depend on the specific problem.

2.2 Osmotic Pressure

Although there are many models of gel dynamics in the literature which include terms representing osmotic pressure [2, 3, 5, 6, 9, 10, 12], there is little agreement on either the definition or the derivation of this term. The treatment of this term varies from qualitative [3, 5] to quantitative [12]. In [6, 9, 10] a specific functional form of the osmotic pressure is not given. In fact, there has been little investigation of the dynamic behavior using different forms of the swelling pressure. Therefore our first task is to derive a model of swelling pressure which reflects some experimental results. Specifically, in many experiments a blob of gel is suspended in a solvent causing the gel to swell. The amount of swelling is a measure of the effectiveness of the solvent. In general, the gel does not completely dissolve, instead

the blob swells a certain amount and then persists with a lower volume fraction, maintaining a distinct interface between the gel and the surrounding solvent. We wish to determine what choice of Ψ, if any, allows for the existence of an edge between the gel and the surrounding solvent.

Implications of the form of the osmotic pressure can be seen from analysis of a simplified one dimensional model of network redistribution due to swelling pressure. In the absence of frictional interaction ($h_f = 0$) and elastic restoring force ($\sigma_e = 0$), network motion is governed by the balance of forces due to viscous stress, osmotic pressure and hydrostatic pressure. Once the network and solvent velocities are uncoupled we can take $\vec{U}_s = 0$ which implies that $\nabla P = 0$, from equation 4. If we further assume that equation 2 depends only on x, we obtain equations which we use to motivate our choice of Ψ. Assuming that θ_n and $\vec{U}_n$ are time independent in equation 4, the steady, one-dimensional equations governing the network distribution are

$$\eta \frac{d}{dx}(\theta_n \frac{dV_n}{dx}) = \frac{d}{dx}\Psi(\theta_n), \tag{7}$$

$$\frac{d}{dx}(\theta_n V_n) = \epsilon \frac{d^2\theta_n}{dx^2}, \tag{8}$$

where V_n is the x-component of $\vec{U}_n$. We have introduced the term $\epsilon \frac{d^2\theta_n}{dx^2}$ in equation 8 to smooth out sharp interfaces in the network distribution assuring that the solutions are C^∞. For the solutions to be physically reasonable the solution should persist in the limit $\epsilon \to 0$.

We take $\Psi(\theta_n) = \gamma_{os}{\theta_n}^2(\theta_n - \theta_{ref})$, where θ_{ref} is a reference volume fraction. Our goal is to show that the proposed form of the osmotic pressure yields a transition layer between two different network volume fractions, zero and a reference value. This is a necessary feature of our model since, in general, gels do not dissolve when submerged in a poor solvent. Instead the gel swells, but the 'edge' of the gel is still evident.

We nondimensionalize these equations by setting $\hat{V} = V/V_0$, $\hat{x} = x/L$, $\Psi(\theta_n) = \hat{\Psi}/\gamma_{os}$where $V_0 = \frac{L\gamma_{os}}{\eta}$ is a velocity scale, L is the length of the domain, which assumed to be finite. Substituting these into the above equations collecting all of the scaling parameters into $\hat{\epsilon} = \frac{\epsilon}{V_0 x_0}$ and $\hat{\eta} = \frac{\eta V_0}{L\gamma_{os}} = 1$ and dropping the nondimensional 'hat' notation yields the nondimensional

equations

$$\frac{d(\theta_n \frac{dV_n}{dx})}{dx} = \frac{d\Psi(\theta_n)}{dx}, \tag{9}$$

$$\frac{d\theta_n V_n}{dx} = \epsilon \frac{d^2\theta_n}{dx^2}. \tag{10}$$

To conserve θ_n, we require $\frac{d\theta_n}{dx} = \theta_n V_n$ at $x = 0$ and1 (i.e. no-flux) . We also require the velocity to be zero at the boundary. Integrating equations 9 and 10, and applying the boundary conditions yields

$$\frac{dV_n}{dx} = \theta_n(\theta_n - \theta_{ref}) + \frac{k_1}{\theta_n}, \tag{11}$$

$$\frac{d\theta_n}{dx} = \frac{\theta_n V_n}{\epsilon}, \tag{12}$$

since $\Psi(\theta_n) = \theta_n^2(\theta_n - \theta_{ref})$.

We seek solutions of this system which have a sharp transition layer between $\theta_n = 0$ and $\theta_n = \theta_{ref}$ by requiring $(\theta_n, V_n) = (0, 0)$ and $(\theta_n, V_n) = (\theta_{ref}, 0)$ to be critical points of the system which implies $k_1 = 0$. We then construct a heteroclinic trajectory connecting the two critical points by solving

$$\frac{dV_n}{d\theta_n} = \epsilon \frac{\theta_n - \theta_{ref}}{V_n}. \tag{13}$$

This equation is separable and has solution

$$\frac{V_n^2}{2} = \epsilon(\frac{\theta_n^2}{2} - \theta_{ref}\theta_n) + k_3. \tag{14}$$

For this trajectory to be a heteroclinic connection the velocity must vanish at $\theta_n = \theta_{ref}$, so $k_3 = \frac{\epsilon\theta_{ref}^2}{2}$. Therefore the trajectories are $V_n = \pm\sqrt{\epsilon}(\theta_n - \theta_{ref})$ and since

$$\frac{d\theta_n}{dx} = \frac{\theta_n V_n}{\epsilon}, \quad = \pm\frac{\theta_n(\theta_n - \theta_{ref})}{\sqrt{\epsilon}}, \tag{15}$$

the trajectory is flat near $\theta_n = 0$ and $\theta_n = \theta_{ref}$. This argument can be extended to show that edged solutions exist for $\Psi(\theta_n)$ of the general form $\Psi(\theta_n) = \theta_n^2 f(\theta_n)$, where $f(\theta_{ref}) = 0$ and $f(\theta_n) < 0$ for $\theta_n < \theta_{ref}$.

Having determined that the form of the osmotic pressure specified above yields steady solutions consisting of transition layers between $\theta_n = 0$ and $\theta_n = \theta_{ref}$ we now wish to determine how these steady solutions may arise.

Notice that any constant θ_n is a solution of equations 9 and 10 with $V_n = 0$. In the following we determine the stability of the constant solutions by considering the associated dynamic problem

$$\frac{\partial}{\partial x}(\theta_n \frac{\partial V_n}{\partial x}) = \frac{\partial \Psi(\theta_n)}{\partial x}, \tag{16}$$

$$\frac{\partial \theta_n}{\partial t} + \frac{\partial}{\partial x}(\theta_n V_n) = \epsilon \frac{\partial^2 \theta_n}{\partial x^2}. \tag{17}$$

Linearizing these equations about the constant steady-state solutions, i.e $\theta_n = \theta_0 + \phi(x,t)$ and $V_n = V_{n0} + u$ yields the linear system,

$$\frac{\partial}{\partial x}(\phi \frac{\partial V_{n0}}{\partial x} + \theta_0 \frac{\partial u}{\partial x}) = \Psi' \frac{\partial \phi}{\partial x}, \tag{18}$$

$$\frac{\partial \phi}{\partial t} + \frac{\partial}{\partial x}(\phi V_{n0} + \theta_0 u) = \epsilon \frac{\partial^2 \phi}{\partial x^2}. \tag{19}$$

To determine the stability of the steady solutions, we assume that $\phi(x,t) = e^{\lambda t}\Phi(x)$ and determine the sign of the real part of λ. Under these assumptions the above system reduces to

$$\theta_0 \frac{\partial^2 u}{\partial x^2} = \Psi' \frac{\partial \Phi}{\partial x} \tag{20}$$

$$\lambda \Phi + \theta_0 \frac{\partial u}{\partial x} = \epsilon \frac{\partial^2 \Phi}{\partial x^2}. \tag{21}$$

Because the domain is the interval $(0,1)$, we assume a solution of the form $u(x) = A_1 \cos(n\pi x) + B_1 \sin(n\pi x)$ and $\Phi(x) = A_2 \cos(n\pi x) + B_2 \sin(n\pi x)$. The boundary conditions, $u = \frac{\partial \Phi}{\partial x} = 0$, imply that $A_1 = B_2 = 0$ and equations 20 and 21 reduce to a matrix equation

for the constants B_1 and A_2

$$-(n\pi)^2\theta_0 B_1 + n\pi\Psi' A_2 = 0 \quad (22)$$

$$n\pi\theta_0 B_1 + (\lambda + \epsilon(n\pi)^2)A_2 = 0. \quad (23)$$

For nontrivial solutions to this equation to exist the determinant of the coefficient matrix must vanish, so that

$$\lambda = -(\epsilon(n\pi)^2 + \Psi'(\theta_0)). \quad (24)$$

In the limit $\epsilon \to 0$, the stability depends on the sign of Ψ'. If the sign of $\Psi'(\theta_0)$ is positive the solution is stable and if it is negative the solution is unstable. Thus fro the function $\Psi(\theta_n) = \gamma_{os}\theta_n^2(\theta_n - \theta_{ref})$, a uniform gel with $\theta_n < \gamma_{os}\frac{2}{3}\theta_{ref}$ is unstable and will self-compress while a uniform gel with $\theta_n > \gamma_{os}\frac{2}{3}\theta_{ref}$ is stable.

3 Channeling in a Gel-Poiseulle Flow

We now turn to a simple flow problem illustrating one difference between gel dynamics and Newtonian fluid dynamics. We consider the motion of a gel between two flat plates with a constant imposed pressure drop.

The motion is assumed to be two-dimensional where x, y and $\vec{U}_* = (V_*, W_*)$ denote the horizontal and vertical coordinates and velocities respectively. For Newtonian fluids the steady-state x-independent velocity profile is parabolic in y for all pressure drops. This is not the case for the gel-Poiseulle flow. Instead, the steady-state profile of the network volume fraction undergoes a large change as the magnitude of the pressure gradient varies.

To demonstrate this, we seek a solution of equations 2 through 6 that is the analog of Poiseulle flow - the horizontally independent, steady velocity profile for a fluid forced between two flat plates by a pressure drop.

Under the assumption that D_1 and D_2 are independent of x, the elements of the defor-

mation gradient tensor $\mathbf{F}_{ij}$ are

$$\begin{aligned}
\frac{\partial x'}{\partial x} &= 1, \\
\frac{\partial x'}{\partial y} &= \frac{\partial D_1}{\partial y}, \\
\frac{\partial y'}{\partial x} &= 0, \\
\frac{\partial y'}{\partial y} &= 1 + \frac{\partial D_2}{\partial y},
\end{aligned}$$

and the stress tensor becomes

$$\sigma_n = \gamma \begin{bmatrix} 0 & \frac{\partial D_1}{\partial y} \\ \frac{\partial D_1}{\partial y} & \frac{\partial D_1}{\partial y}^2 + 2\frac{\partial D_2}{\partial y} + \frac{\partial D_2}{\partial y}^2 \end{bmatrix}.$$

We change from vector to component notation here, so that the following simplifications are more apparent. In component form the steady-state equations for the gel-Poiseulle flow are

$$\eta \frac{\partial}{\partial y}(\theta_n \frac{\partial}{\partial y} V_n) - \frac{\partial P}{\partial x} + \gamma \frac{\partial}{\partial y}(\theta_n \frac{\partial}{\partial y} D_1) = 0, \tag{25}$$

$$\begin{aligned}
\eta \frac{\partial}{\partial y}(\theta_n \frac{\partial}{\partial y} W_n) - \frac{\partial}{\partial y}\Psi(\theta_n) - \frac{\partial P}{\partial y} \\
+\gamma \frac{\partial}{\partial y}(\theta_n (\frac{\partial D_1}{\partial y}^2 + 2\frac{\partial D_2}{\partial y} + \frac{\partial D_2}{\partial y}^2)) &= 0,
\end{aligned} \tag{26}$$

$$h_f \theta_n (V_n - V_s) - \frac{\partial P}{\partial x} = 0, \tag{27}$$

$$h_f \theta_n (W_n - W_s) - \frac{\partial P}{\partial y} = 0, \tag{28}$$

$$\frac{\partial}{\partial y}(\theta_n W_n + (1 - \theta_n) W_s) = \epsilon \frac{\partial^2 \theta_n}{\partial y^2} \tag{29}$$

$$\frac{\partial}{\partial y}(\theta_n W_n) = \epsilon \frac{\partial^2 \theta_n}{\partial y^2}, \tag{30}$$

$$\frac{\partial}{\partial y}(D_1 W_n) = V_n, \tag{31}$$

$$\frac{\partial}{\partial y}(D_2 W_n) = W_n. \tag{32}$$

Here we allow for network diffusion, with diffusion coefficient ϵ but our goal is to solve the system in the limit $\epsilon \to 0$.

The distance between the two plates is taken to be L, hence the domain of the problem consists of an infinite strip $(-\infty < x < \infty) \times (0 < y < L)$. The boundary conditions are $D_1 = D_2 = 0$ and $\epsilon \frac{\partial \theta_n}{\partial y} = \theta_n W_n$ at $y = 0, L$, implying that there is neither network movement nor network flux at the boundary.

We can simplify these equations substantially. Integrating equation 30 and solving for the vertical velocity of the network we find

$$W_n = \epsilon \frac{\frac{\partial \theta_n}{\partial y} + c_1}{\theta_n}, \tag{33}$$

which combined with equation 29 yields

$$(1 - \theta_n) W_s = c_2. \tag{34}$$

These can be used in equation 28 to solve for the $\frac{\partial P}{\partial y}$ as

$$\frac{\partial P}{\partial y} = h_f \theta_n (W_n - \frac{c_2}{1 - \theta_n}). \tag{35}$$

The boundary conditions imply that $c_1 = c_2 = 0$, hence $W_s = 0$ and $\frac{\partial P}{\partial y} = h_f \epsilon \frac{\partial \theta_n}{\partial y}$. Because $V_n = 0$ at steady-state, and the equations are independent of x, $\frac{\partial P}{\partial x}$ is independent of x. That is, equation 27 implies that $P = Gx + \hat{P}(y)$.

Integrating equation 25 and solving for $\frac{\partial D_1}{\partial y}$ yields

$$\frac{\partial D_1}{\partial y} = \frac{Gy + a}{\gamma \theta_n}. \tag{36}$$

We specify a by assuming that the steady-state profiles are symmetric about the center line, $y = \frac{1}{2}$. We also relate the vertical displacements to the network volume fraction using the Jacobian of the transformation

$$\hat{\theta}_n = \theta_n (1 + \frac{\partial D_2}{\partial y})$$

where $\hat{\theta}_n$ is the original homogeneous distribution of the network.

Finally, equation 26 reduces to an ordinary differential equation relating the volume fraction of the network to y and parameters G, γ, h_f, etc.

$$\begin{aligned} \epsilon\eta\frac{d}{dy}\left(\theta_n\frac{d}{dy}(\frac{\frac{d\theta_n}{dy}}{\theta_n})\right) - \epsilon h_f\frac{d\theta_n}{dy} \\ -\frac{d\Psi}{dy} + \gamma\frac{d}{dy}\left(\theta_n(\left(\frac{Gy - GL/2}{\gamma\theta_n}\right)^2 + (\frac{\hat{\theta}_n}{\theta_n})^2 - 1)\right) &= 0 \end{aligned} \tag{37}$$

We nondimensionalize equation 37 by defining the nondimensional terms $\epsilon^* = \frac{L^2\eta}{\gamma}\epsilon$ and $h_f^* = \frac{h_f}{L^2\eta}$, substituting these into equation 37, dropping the $*$-notation and integrating once yields

$$\begin{aligned} \epsilon\left(\theta_n\frac{d}{dy}(\frac{\frac{d\theta_n}{dy}}{\theta_n})\right) - \epsilon h_f\theta_n - \Psi(\theta_n) \\ +\left(\theta_n((\frac{Gy - G/2}{\theta_n})^2 + (\frac{\hat{\theta}_n}{\theta_n})^2 - 1)\right) &= k, \end{aligned} \tag{38}$$

which must be solved subject to the constraint that mass is conserved

$$\int_0^1 \theta_n \, dy = \hat{\theta}_n. \tag{39}$$

Although simpler than the original system, there is quite a lot of structure in Equation 38. In particular, Equation 38 is a second order ODE which is singular in the limit $\epsilon \to 0$ (i.e. no network diffusion). The outer equation ($\epsilon = 0$), is an algebraic equation relating the network volume fraction to the location between the plates. In the outer region, the steady state network profile is given by the solution of the algebraic equation and the profile depends on the pressure drop G and the integration constant k. We find that for some values of G, there is a non-functional relationship between these which suggests the existence of interior layers for some parameter values. In the following section we describe the transition layer solution of equation 38.

4 The Channeling Bifurcation

In this section we analyze the bifurcation structure of channels by examining the solutions of equation 38 in the singular limit $\epsilon \to 0$. We assume that the initially uniform gel at $\hat{\theta_n}$ is stable so that $\Psi'(\hat{\theta_n}) > 0$. Setting $\epsilon = 0$, we find that the solution profile $\theta_n(y)$ must satisfy the equation

$$H(y, \theta_n) = G^2(y - 1/2)^2 + h(\theta_n) = 0, \tag{40}$$

where

$$h(\theta_n) = -\theta_n \Psi(\theta_n) + \theta_n \Psi(\hat{\theta_n}) + \hat{\theta_n}^2 - \theta_n^2 - k\theta_n. \tag{41}$$

Here k has been redefined so that $H(\hat{\theta_n}) = 0$ when $k = 0$.

Finally, the solution profile $\theta_n(y)$ must satisfy the integral constraint

$$\int_0^1 \theta_n(y) dy = \hat{\theta_n}. \tag{42}$$

We assume

$$\Psi(\theta_n) = \kappa\theta_n^2(\theta_n - \theta_{ref}) \tag{43}$$

where $\kappa = \frac{\gamma_{os}}{\gamma}$ represents the strength of osmosis compared to the elastic modulus. Thus, the gel is capable of supporting an edge.

First we make some observations about the function $h(\theta)$. Because $h(0) = \hat{\theta_n}^2 > 0$, and $h(\theta_n) < 0$ for large θ_n, there is always at least one positive and one negative root. Since $h(\theta)$ is a quartic polynomial, there can be as many as three positive roots of $H(y, \theta_n) = 0$ depending on the value of k. To see this, in figure 1 are shown four different plots of $h(\theta_n)$ for four values of $k = 0, 2, 3.5, 5$ (top to bottom).

If $3\kappa\theta_{ref}^2 > 8$, then the function $h(\theta_n)$ has two positive inflection points. Without inflection points the solution of $H(y, \theta_n) = 0$ is unique for all y. Otherwise there is the possibility of profiles with interior layers. Thus, interior layer solutions exist only if κ is sufficiently large.

If there exists a value of y, say y_0 for which $H(y_0, \theta_n)$ does not have a unique solution, we introduce an inner scaling of equation 38 defining $y^* = \frac{y - y_0}{\epsilon^{1/2}}$. Substituting this into equation

38, dropping the y^* notation and taking the leading order terms we obtain

$$\begin{aligned} & \frac{d}{dy}\left(\frac{\frac{d\theta_n}{dy}}{\theta_n}\right) - \Psi(\theta_n)/\theta_n \\ + & \left(\left(\frac{Gy_0 - G/2}{\theta_n}\right)^2 + \left(\frac{\hat{\theta}_n}{\theta_n}\right)^2 - 1 \right) \quad = \quad k\theta_n. \end{aligned} \tag{44}$$

By the change of variable $w = \ln(\theta_n)$, we can simplify this to

$$\frac{\partial^2 w}{\partial y^2} + F(w; G, y_0) = 0, \tag{45}$$

where $F(w; G, y_0) = \Psi(e^w)e^{-w} + \left(\left(\frac{Gy_0 - G/2}{e^w}\right)^2 + \left(\frac{\hat{\theta}_n}{e^w}\right)^2 - 1 \right) - ke^{-w}$. There exists a solution [4] to the inner-layer equation 45 if F has three positive roots, $w_- < w_0 < w_+$ and if

$$\int_{w_-}^{w_+} F dw = 0. \tag{46}$$

Inverting the transformation yields an equivalent requirement in the variable θ_n. An interior layer will be fit at $y = y_0$ if $H(y_0, \theta_n) = 0$ has three positive roots, say $\theta_- < \theta_0 < \theta_+$, and if

$$\int_{\theta_-}^{\theta_+} \frac{H(y_0, \theta_n)}{\theta_n^3} d\theta_n = 0. \tag{47}$$

Otherwise the profile will not have a boundary layer.

The most convenient way to solve this problem is to fix k and to find the corresponding values of G and y_0 (if any) for which solutions exist. If $h(\theta^*) = 0$ and $h(\theta_n)$ is monotone decreasing for $\theta_n > \theta^*$, then there is a unique solution of $H(y, \theta_n) = 0$, for any value of G as seen in figure 1 with $k = 2$ and for $k = 5$. In figure 2 the solution profiles $\theta_n(y)$ for $k = 5$ are shown for three different values of G.

Moreover, since G acts as a y-axis scale factor for these profiles it is apparent that $\int_0^1 \theta_n(y)dy$ is a monotone decreasing function of G. Thus, it is easy to find the unique value of G for which $\int_0^1 \theta_n(y)dy = \hat{\theta}_n$. For the profiles shown in figure 2, this unique value of G is

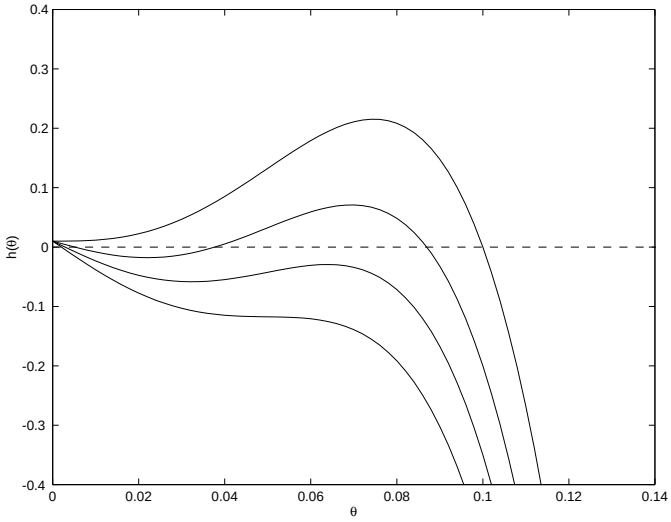

Figure 1: Plot of $h(\theta)$ as a function of θ for $k = 0, 2, 3.5, 5$. Other parameter values are $\kappa = 20,000$, $\theta_{ref} = \hat{\theta}_n = 0.1$.

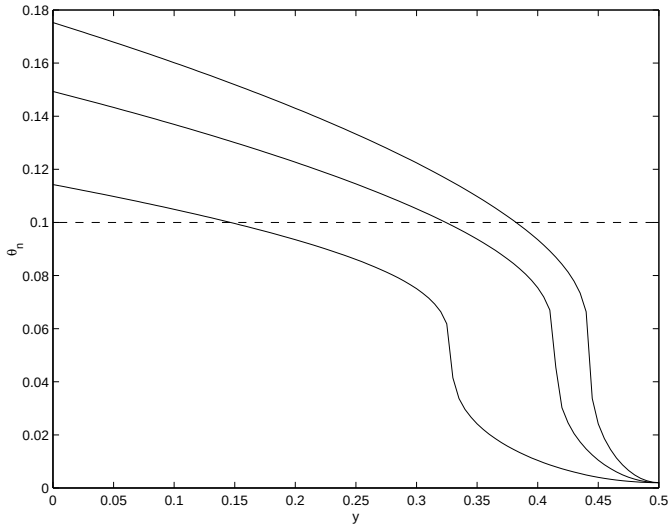

Figure 2: Plot of $\theta_n(y)$ for $k = 5$ and $G = 2, 4.022, 6$. Other parameter values are $\kappa = 20,000$, $\theta_{ref} = \hat{\theta}_n = 0.1$.

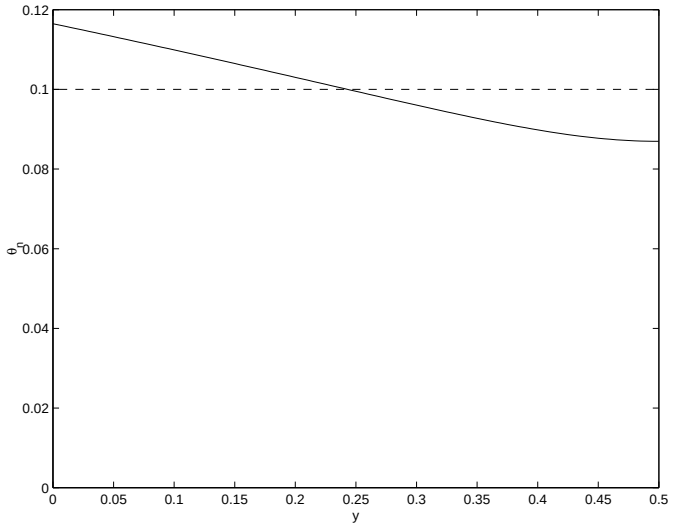

Figure 3: Plot of $\theta_n(y)$ for $k = 2$ and $G = 1.74$. Other parameter values are $\kappa = 20,000$, $\theta_{ref} = \hat{\theta_n} = 0.1$.

4.022.

Similarly, for small values of k, unique solutions can be obtained. For example, figure 3 shows the solution profile for $k = 2$. Again, since the y-axis for this profile is scaled by G, the unique value of G for which $\int_0^1 \theta_n(y)dy = \hat{\theta_n}$ is easily determined. For the profile in figure 3, this value is $G = 1.74$.

If the function $h(\theta_n)$ is not monotone decreasing then there is the possibility of nonunique solutions of $H(y, \theta_n) = 0$. If a (positive) level x can be found so that

$$\int_{\theta_-}^{\theta_+} \frac{x + h(\theta_n)}{\theta_n^3} d\theta_n = 0, \tag{48}$$

then a boundary layer can be inserted into the profile at $y_0 = \frac{1}{2} \pm \frac{\sqrt{x}}{G}$, and this boundary layer can be used to connect the largest solution of $H(y_0, \theta_n) = 0$ with the smallest. A plot of a profile that results is shown in figure 4.

Notice that for this value of k (=2), there are two possible solution profiles, one with no interior layer shown in figure 3, and one with a boundary layer shown in figure 4. These profiles obtain for different values of G. For other values of k, the boundary layer profile is the only possible solution. A profile of this type occurs for $k = 3.5$ and is shown in figure 5.

In this way, for each value of k we determine all possible solutions and their corresponding

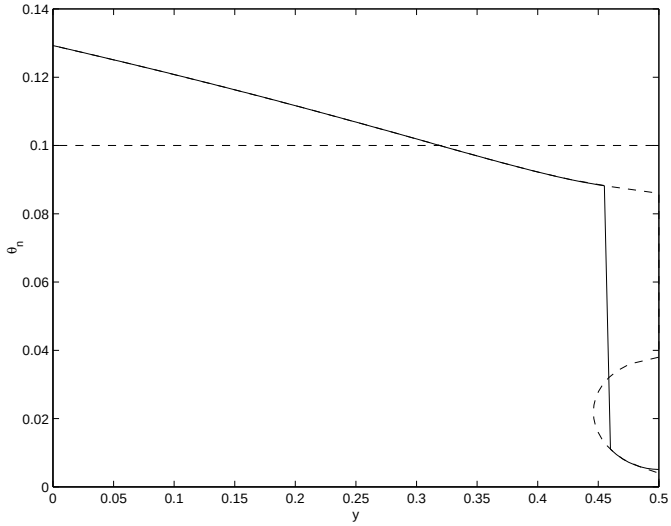

Figure 4: Plot of $\theta_n(y)$ for $k = 2$ and $G = 2.47$ with a boundary layer inserted at $y_0 = 0.46$. The dashed curves shows all possible solutions of $H(y, \theta_n) = 0$. Other parameter values are $\kappa = 20,000$, $\theta_{ref} = \hat{\theta_n} = 0.1$.

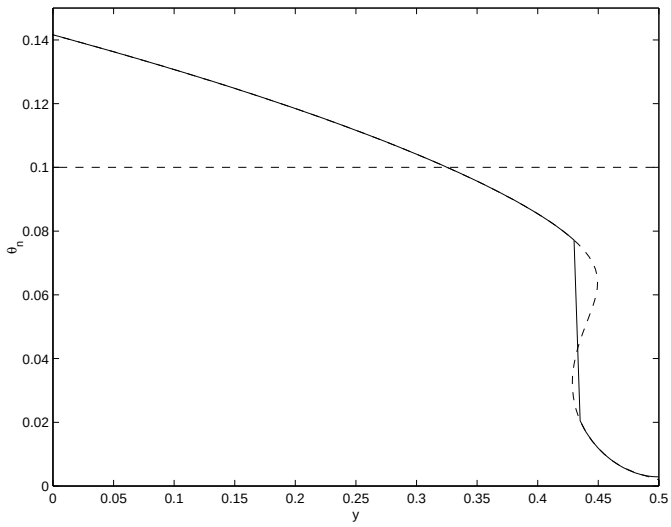

Figure 5: Plot of $\theta_n(y)$ for $k = 3.5$ and $G = 3.39$ with a boundary layer inserted at $y_0 = 0.43$. The dashed curves shows all possible solutions of $H(y, \theta_n) = 0$. Other parameter values are $\kappa = 20,000$, $\theta_{ref} = \hat{\theta_n} = 0.1$.

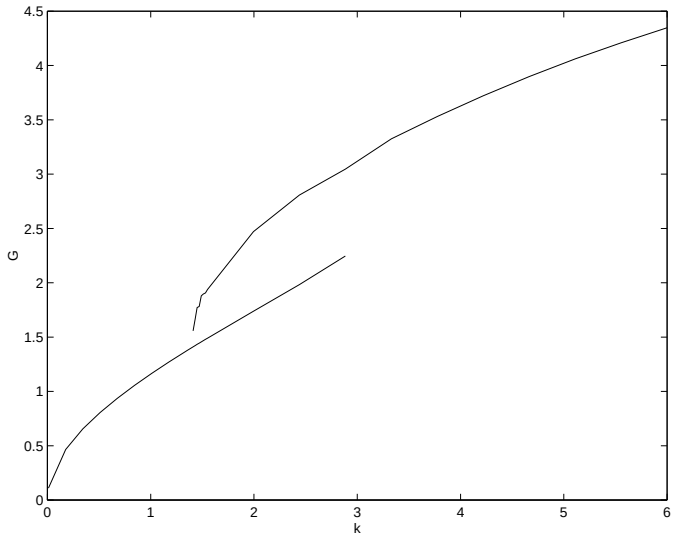

Figure 6: Plot of G vs. k for the solutions of the gel-flow problem. For this plot, $\kappa = 20,000$, $\theta_{ref} = \hat{\theta_n} = 0.1$.

values of G. A plot of the relationship between k and G is shown in figure 6. Here we see two curves. The lower curve that extends from $k = 0$ to $k = 2.9$ corresponds to solutions like those shown in figure 3 , with no boundary layer. The upper curve that bifurcates from the lower curve at about $k = 1.4$ (with $y_0 = \frac{1}{2}$) corresponds to channeled solutions, with a boundary layer as shown in figure 4 and 5 for $k < 5$. These solutions merge smoothly into non-boundary layer solutions such as those shown in figure 2 as k increases.

The significant feature of these two curves is that for some values of G there are two possible solutions, a boundary layer solution and a non-boundary layer solution. Thus, the solution of the gel-flow problem is not unique.

The behavior of the fluid flow through these two different solution types is understandably different, as the channeled solution permits a higher flux for the same cost. This is illustrated by figure7 where the flux of solvent,

$$J = \int_0^1 V_s dy = \frac{1}{h_f} \int_0^1 \frac{1 - \theta_n}{\theta_n} dy \tag{49}$$

is plotted as a function of G for the two different solution types. Not surprisingly, if two solutions are possible for the same value of G, the boundary layer solution permits a larger solvent flux than the non-boundary layer solution.

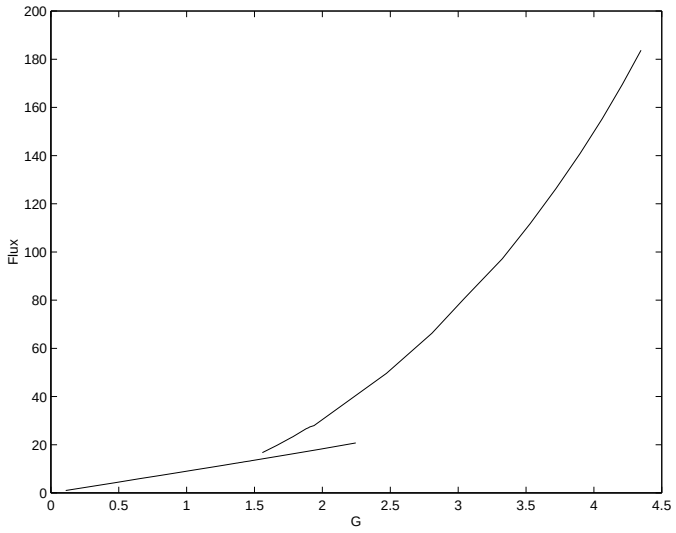

Figure 7: Plot of solvent flux as a function of G. For this plot, $\kappa = 20,000$, $\theta_{ref} = \hat{\theta_n} = 0.1$.

5 Discussion

From this analysis we can deduce the physical mechanism that underlies the formation of channels in a gel. If the osmotic force is sufficiently strong compared to the elastic restoring force, then under sufficiently high pressure gradient, it is energetically favorable to compress the gel near the wall, and swell the gel in the interior, thereby forming a low resistance channel.

This same conclusion is correct for all gels for which there are two stable gel concentrations. That is, if $\Psi(\theta_n)$ is such that $\Psi'(\theta_n) < 0$ for $0 \leq \theta_* < \theta_n < \theta^* < 1$ and is positive elsewhere, then if the uniform gel distribution has $\hat{\theta_n} > \theta^*$ and if the osmotic force is sufficiently strong compared to the elastic force, channels will form under sufficiently high pressure gradient flows. This follows from the analysis of the previous section which relied entirely upon the generic "cubic" shape of the function $\Psi(\theta_n)$, and not on its details. Any function $\Psi(\theta_n)$ with similar structure will lead to the same bifurcation channeling behavior.

This work was supported by the NSF-FRG grant #DMS 0139926

References

[1] R. B. Bird, R. C. Armstrong, and O. Hassager, *Dynamics of Polymeric Liquids*, vol. 1, John Wiley and Sons, New York, 1987.

[2] N. G. Cogan and J. P. Keener, *The role of the biofilm matrix in structural development*, Mathematical Medicine and Biology, (2003). Accepted March, 2004.

[3] X. He and M. Dembo, *On the mechanics of the first cleavage division of the sea urchin egg*, Experimental Cell Research, 233 (1997), pp. 252–273.

[4] J. P. Keener, *Principles of applied mathematics: transformation and approximation*, Addison Wesley, Advanced Book Program, 1988.

[5] S. Lubkin and T. Jackson, *Multiphase mechanics of capsule formation in tumors*, Journal of Biomechanical Engineering-Transactions of the ASME, 124 (2002), pp. 237–243.

[6] S. T. Milner, *Dynamical theory of concentration fluctuations in polymer-solutions under shear*, Physical Review E, 48 (1993), pp. 3674–3691.

[7] M. Strathmann, T. Griebe, and H.-C. Flemming, *Agarose hydrogels and eps models*, Water Science and Technology, 43 (2001), pp. 169–175.

[8] H. Tanaka, *Viscoelastic model of phase separation*, Physical Review E, 56 (1997), pp. 4451–4462.

[9] ——, *Viscoelastic phase separation*, J. Phys.: Condens. Matter, 12 (2000), pp. R207–R264.

[10] T. Tomari and M. Doi, *Hysteresis and incubation in the dynamics of volume transitions of spherical gels*, Macromolecules, 28 (1995), pp. 8334–8343.

[11] J. Wingender, T. R. Neu, and H.-C. Flemming, eds., *Microbial Extracellular Polymeric Substances. Characterization, Structure and Function*, Springer, 1999.

[12] C. Wolgemuth, E. Hoiczyk, D. Kaiser, and G. Oster, *How myxobacteria glide*, Current Biology, 12 (2002), pp. 369–377.

[13] C. W. Wolgemuth, E. Hoiczyk, and G. Oster, *How gliding bacteria glide*, Biophysical Journal, 82 (2002), p. 1956.